International Journal of Biochemistry and Cell Biology 153 (2022) 106325

Contents lists available at ScienceDirect

International Journal of Biochemistry and Cell Biology

journal homepage: www.elsevier.com/locate/biocel

IFITM3 promotes NiV envelope protein-mediated entry into MDCK cells and interacts with the fusion subunit of the F protein

Wang Xu [a,b], Shou-Wen Du [a,*], Le-Tian Li [b], Xiao-Shuang Shi [b], Jia-Min Wang [b], Ti-Yuan Li [a], Ning-Yi Jin [b,*], Chang Li [b,*]

[a] Second Clinical Medical College of Jinan University, Shenzhen Peoples Hospital, Shenzhen 518000, China
[b] Research Unit of Key Technologies for Prevention and Control of Virus Zoonoses, Chinese Academy of Medical Sciences, Changchun Veterinary Research Institute, Chinese Academy of Agricultural Sciences, Changchun 130122, China

ARTICLE INFO

Keywords:
IFITM3
Nipah Virus
Fusion protein
Virus entry
Interaction

ABSTRACT

IFITM proteins are a host restriction factor with broad-spectrum antiviral activity, but the role in the paramyxovirus entry remains unclear. Nipah virus (NiV) is a zoonotic virus of the *paramyxoviridae* with extremely high lethality. Here, we assessed the role of IFITM3 on NiV G and F glycoprotein-mediated virus entry. Using NiV pseudovirus bearing NiV G and F proteins to infect IFITM3-induced MDCK cells, we found that overexpression of IFITM3 promotes NiV G and F proteins-mediated virus entry. Mechanistically, the subcellular distribution showed that F protein completely co-localized with IFITM3, but G protein does not. Immunoprecipitation further indicated that IFITM3 strongly captures F protein rather than G protein. F protein truncation found that the F1 subunit completely co-localized and captures with IFITM3, but not the F2 subunit. Furthermore, IFITM3 strongly binds to F1 truncations containing fusion peptide (FP), and F1 strongly captures IFITM3 truncation with the intramembrane domain (IMD). Together, the results suggest that IFITM3 can promote NiV G and F proteins-mediated virus entry into MDCK cells, and IFITM3 directly interacts with the F1 subunit of NiV F protein dependent on the former's IMD and the latter's FP, which may occur after incorporation of fusion peptides into the cell membrane following virus fusion activation.

1. Introduction

NiV disease is still one of the severe infectious diseases requiring urgent research and development efforts in the WHO R&D Blueprint 2018 (The, 2018), with no available vaccine or drug for clinical use. NiV is a negative-sense, single-stranded RNA virus, enveloped, belonging to the *paramyxoviridae* subfamily and a member of the *Henipavirus*. The infected people often die due to severe encephalitis and\or respiratory disorders, with the case fatality ratio ranging from 40% to 100% (Hauser et al., 2021). The glycoproteins G and F on the NiV particles surface mainly participate in the virus attachment and entry into host cells, which are the prerequisite for the virus infecting host cells and the main target for vaccine and drug design (Isaacs et al., 2021). Currently, there are two main pathways for NiV entry into host cells, i.e., fusion at the plasma membrane and fusion in endosomal membranes following micropinocytosis (Pernet et al., 2009), both requiring the collaboration of G and F proteins. Briefly, after NiV G protein contacts the receptor Ephrin B2 or Ephrin B3 on the surface of the host cells, more Ephrin B2 or Ephrin B3 will be recruited and bind to the globular head the G protein, leading to conformation change and exposure of the neck domain. The neck domain interacted with the F protein and activated it, resulting in unstable conformation and prefusion (Yeo et al., 2021). Then, the fusion peptide located on the F1 protein was inserted into the host cell membrane, then the HR1 domain located on the F1 subunit moved toward the HR2 domain, finally forming a stable 6-helix structure to complete the virus-cell membrane fusion and release the viral genome into the cytoplasm (Wong et al., 2021; Zamora et al., 2021; Liu et al., 2013).

Interferon inducible transmembrane protein 3 (IFITM3) is a single-transmembrane small molecule protein mainly located in late endosomes and lysosomes, encoded by interferon-stimulated genes. It possesses multiple biological activities, such as regulation of cell cycle, modulates the immune response, and virus entry into host cells (Yanez et al., 2020; Ren et al., 2020; Majdoul and Compton, 2021). The

* Correspondence to: Research Unit of Key Technologies for Prevention and Control of Virus Zoonoses, Chinese Academy of Medical Sciences, Changchun Institute of Veterinary Medicine, Chinese Academy of Agricultural Sciences, Changchun 130122, China.
E-mail addresses: du-guhong@163.com (S.-W. Du), ningyik@126.com (N.-Y. Jin), lichang78@163.com (C. Li).

https://doi.org/10.1016/j.biocel.2022.106325
Received 21 February 2022; Received in revised form 3 October 2022; Accepted 25 October 2022
Available online 28 October 2022

regulation of virus entry into host cells is most widely studied. Many studies have proved that IFITM3 can effectively inhibit the entry of various envelope or no-envelope viruses into host cells, including Ebola virus (EBOV), vesicular stomatitis virus (VSV), Zika virus (ZIKV), Vaccinia virus (VACV) (Guo et al., 2020; Li et al., 2018), but it does not affect the entry of some DNA viruses, such as adenovirus (AdV) and cytomegalovirus (CMV). It even promotes the entry of some viruses, such as human coronavirus OC43 (HCoV-OC43) (Prelli Bozzo et al., 2021).

Nevertheless, the effects of IFITM3 on different members of paramyxovirus, are not completely the same. IFITM3 can restrict the infection of respiratory syncytial virus (RSV) and parainfluenza virus to host cells but does not affect the measles virus and human metapneumovirus (Smith et al., 2019; Meischel et al., 2021). The Newcastle disease virus (NDV) effect on host cells is unclear (Lv et al., 2019). NiV is one of the few fatal viruses in the paramyxoviridae. There is no study on the influence of interferon-induced transmembrane protein on NiV. Thus, we explored the role of IFITM3 in NiV infection to host cells and elucidated the mechanism, laying a foundation for understanding the infection mechanism and broadening the application of IFITM3.

Given that the study of NiV requires a Biosafety Level 4 (BSL-4) laboratory, the effect of IFITM3 on the NiV G and F proteins-mediated virus entry was investigated by constructing Nipah pseudoviruses (NiVpv) (Nie et al., 2019), and the regulation of IFITM3 on pseudovirus infection capability was assessed by detecting intracellular luciferase activity and the molecular mechanism of IFITM3 in the NiV G and F proteins-mediated virus entry was explored by confocal microscope and immunocoprecipitation (IP), providing a basis for in-depth study of the interaction pattern between IFITM3 and virus.

2. Materials and methods

2.1. Cell lines

All cells in this study were grown in Dulbecco's modified Eagle's medium (DMEM, Sigma, USA) supplemented with 10% fetal bovine serum (Gibco, USA) and 1% penicillin-streptomycin (HyClone, USA), at 37 ℃ with 5% CO_2. The inducible MDCK-Tet3G-IFTTM3 cells derived from the Madin Darby Canine Kidney (MDCK) cells were cultured in DMEM complete medium containing G418 (Gibco, 800 μg/ml, USA) and puromycin (InvivoGen, 4 μg/ml, USA), as described previously (Cao et al., 2017).

2.2. Plasmids

The sequences of G and F genes of Nipah virus (GenBank: AF212302.2) were optimized and synthesized by GenScript, and cloned into the mammalian cell expression vector pCAGGS, named pCAGGS-G and pCAGGS-F, respectively. In this study, the G genes or F genes and their truncates inserted into the pEGFP-N3 vector were cloned by PCR reaction using pCAGGS-G or pCAGGS-F as the template. We constructed plasmids expressing IFITM3 or its truncates, and the plasmids carrying organelle marker genes were purchased from Sino Biological.

The backbone plasmid pCMV4.3-Luc for packaging pseudoviruses is an upgraded version of the first generation lentivirus-packaging system backbone plasmid pNL4.3-R$^-$E$^-$. Luc. Briefly, using the In-Fusion method (TAKARA, Japan), the CMV promoter from the pcDNA3.1 vector was inserted before the luciferase (Luc) element of the pNL4.3-R$^-$E$^-$. Luc and the restriction sites were *Not* I and *Xho* I. Use *Stbl*3 chemically competent *E.*coli cells (TransGen Biotech, China) to produce this plasmid, named pCMV4.3-Luc. All of the sequences were confirmed by DNA sequencing.

2.3. Production Nipah pseudovirus

Nipah pseudoviruses were produced by using a lentivirus packaging system. 239 T cells were seeded and cultured in a six-well plate overnight until 60%−70% confluence on the day prior to transfection. Before transfection, the medium was replaced with the fresh Opti-MEM Medium (Gibco, USA), 1 ml/well. According to the lipofectamine™3000 transfection reagent user's instruction manual (Invitrogen, USA), the plasmid pCAGGS-G、pCAGGS-F、pCMV4.3-Luc were co-transfected into 293 T cells with the ratio 2:1:3, then incubated at 37 ℃ for 6 h. Afterward, remove the transfection mixture and replace it with 2 ml/well of growth medium with 2% FBS. Forty-eight hours post-transfection, NiVpv in culture supernatants were harvested, centrifuge at 8,000 rpm/min for 5 min to remove the cell debris, filtered with a 0.45 μm low protein binding filter and stored at −80 ℃ in 2 ml micro-centrifuge tube.

2.4. Virus infection detection

In vitro, seeding the target cells into a 96-well plate and cultured overnight at 37 ℃, 2×10^4 live cells/well. Discard the original medium, add the virus solution, 100 μl/well. Place the plate in the cell incubator for 2 h, then discard virus, add complete culture medium and continue culturing to 48 h. Then add the One-Lumi™ Firefly Luciferase Assay reagent (Beyotime), 100 μl/well, incubate 5 min at room temperature, using a multimode microplate reader (TECAN, Switzerland) to read the fluorescence signal intensity. In vivo, mice were anesthetized by IP injection of 1.25% 2,2,2-Tribromoethanol (0.2 ml/10 g body weight), followed by an IP injection of D-luciferin (Promega, USA), then detected the bioluminescence signal using the IVIS-Lumina III imaging system (PerkinElmer, USA).

2.5. Transmission electron microscopy

TEM was utilized to observe the virus particles. After 293 T cells were transfected for 48 h, the viral supernatants were centrifuged at 25,000 rpm for 2 h in a Beckman Type 70Ti rotor at 4 ℃ through a 20% sucrose cushion. The supernatants were discarded and the viral pellet was suspended in PBS solution. Samples were loaded onto carbon-coated Cu grids (ZXBR, China) then dyed using 0.25% phosphotungstic acid (ZXBR, China), and observed by using the Transmission Electron Microscopy (Hitachi, Japan).

2.6. Subcellular localization

BHK cells were seeded on 12 well glass bottom plates (Cellvis, USA), 3×10^5 lives cells/well. Overnight, cells were transfected with a total of 3 μg of different plasmids using PEIpro (Polyplus, France) according to the manufacturer's protocol. Forty-eight hours after transfection, cells were washed with PBS and fixed in 4% polyoxymethylene (Beyotime, China) for 10 min at room temperature, then stained the nucleus with DAPI. A laser confocal microscope were used to take pictures, which then were analyzed with ImageJ software.

2.7. Co-IP and western blot

293 T cells were seeded in six-well plates. Overnight, cells were transfected with a total of 4 μg of various plasmids using PEIpro. Forty-eight hours later, the cells were collected to a centrifuge tube and centrifuged at 5,000 rpm for 5 min at 4 ℃. Using the cell lysis buffer for Western blot and IP (Beyotime, China) to resuspend the cell pellet and place it on ice for at least 30 min. Then centrifuged at 12,000 rpm for 5 mins at 4 ℃ and transferred the supernatant to a new tube for Co-IP experiments. According to the user manual, the equilibrated magnetic beads (Alpalife, china) were added to the cell lysates, then incubated with rotation for 2 h at 4 ℃. The beads were pelleted down using a magnetic rack and washed five times with the PBS buffer. Then using 1 ×SDS loading buffer to elute the proteins bound to the magnetic beads for 10 min at 96 ℃. Then the eluate and input cell extract samples were analyzed by polyacrylamide gel electrophoresis (SDS-PAGE) and

transferred onto nitrocellulose filter (NC) membranes (Cytiva, USA). NC membranes were blocked in 5% skimmed milk/TBST (BD, USA) for 1 h at RT and then incubated overnight with primary antibodies. Membranes were washed three times using TBST and incubated with second antibodies for 1 h at RT. Chemiluminescent signals were measured with the FluorChem E (Proteinsimple, USA).

2.8. Data presentation and statistical analysis

Quantitative data were shown as the mean ± standard deviation of usually 3–5 independent experiments. T-test was processed using the Prism 5.0c software (GraphPad, USA). *p*-values < 0.05 or 0.01 were considered statistically significant.

3. Results

3.1. Construction and identification of Nipah pseudoviruses

Given that the experiment of NiV needs to be performed in a BSL-4 laboratory, NiV glycoprotein enveloped pseudotyped virus (NiVpv) was constructed using a lentivirus vector. Briefly, the plasmids carrying NiV *G* and *F* genes, as well as lentivirus-based packaging system plasmids (pCMV4.3-Luc), were co-transfected into 293 T cells (Fig. 1A). After 48 h of transfection, a lot of cells became larger in the virus packaging cells, similar to the syncytium structure formed by NiV-infected cells (Welch et al., 2018; Chua et al., 2007), compared with transfected cells with only pCMV4.3-Luc (Fig. 1B). Total cellular protein was extracted from the cells to identify the pseudovirus packaging system. The culture supernatants were collected and concentrated by PEG. Then, a small amount of the concentrated product was used to identify the pseudotyped virus components, using β-actin and HIV p24 protein as internal references. Western blot results indicated that NiV G and full-length F (F0) proteins were highly expressed in cells, and F0 protein was cleaved into F1 and F2 (not shown in the figure). G protein, F0 protein, and weak F1 protein subunit bands were detected in the pseudotyped virus extract, suggesting that NiV G and F proteins-enveloped pseudotyped virus was obtained (Fig. 1C). After negative staining, spherical particles with a diameter of about 150 nm were observed under an electron microscope, with obvious spikes on the surface (Fig. 1D) and a similar shape as real NiV (Chua et al., 2007).

After 48 h of HEK293 cells infected with NiVpv, the result of luciferase activity indicated that the cells infected with the pseudovirus expressed luciferase, which was reacted with its substrate to produce a strong fluorescence signal (Fig. 1E), suggesting that NiVpv could be used in cell infection studies. In addition, the infection of NiVpv to mice was also assessed. In vivo imaging system of mice presented obvious fluorescence at the abdomen after 48 h of infection with NiVpv via the intraperitoneal injection (Fig. 1F), indicating that NiVpv infection study is feasible in mice.

3.2. IFITM3 can promote NiVpv infection in MDCK cells

MDCK-Tet3G-IFITM3, the IFITM3-induced expression cell line based on the Tet-On 3 G system previously constructed by our team (Cao et al., 2017), was used to analyze the impact of IFITM3 on NiV G and F proteins-mediated virus entry. The cells were confirmed first. The results

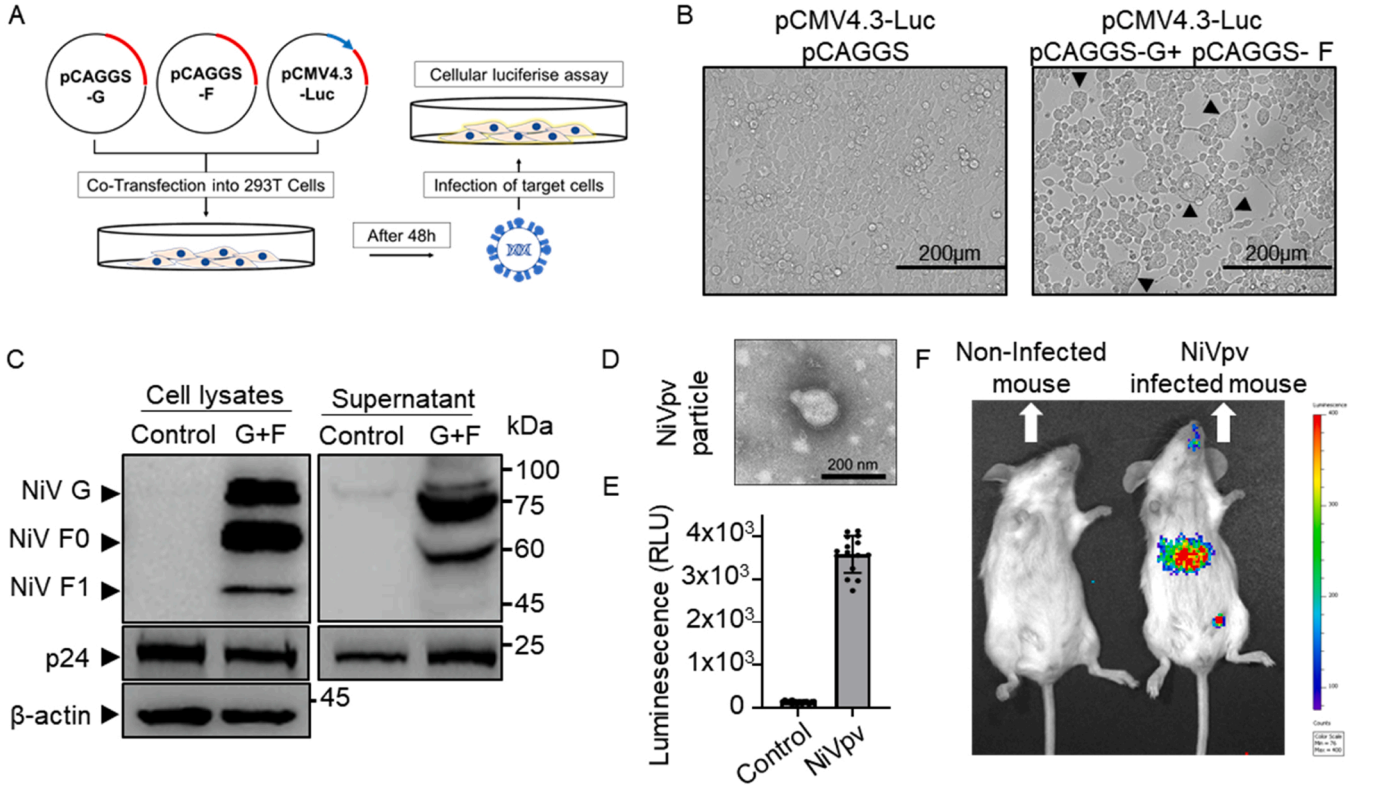

Fig. 1. Nipah pseudovirus production and appraisal. (A) Schematic representation of NiV pseudovirus production. The HEK 293 T cells were used to produce Nipah pseudovirus, then test them with HEK293 cells. (B) Some giant cells (black triangles) appeared in the 293 T cells co-transfected with the plasmids pCAGGS-G、pCAGGS-F and pCMV4.3-Luc compared with only transfected cells with pCMV4.3-Luc. (C) After transfecting plasmids, 48 h, the NiV G、F and HIV-1 p24 proteins could be tested by Western blot in the cell lysates and the medium supernatant with anti-Myc tag antibody (CST, USA) and anti-HIV p24 antibody (Sino Biological, china). (D) The cell culture supernatant used to produce the Nipah pseudovirus was subjected to ultracentrifugation, and Nipah pseudovirus particles were observed in the pill using TEM (Transmission Electron Microscope) dyeing with phosphotungstic acid. The diameter is about 150 nm. Scale bar: 200 nm. (E) The relative luminescence intensity (RLU) of the cells infected with Nipah pseudovirus for 48 h was more than 10^3 times that of uninfected cells. (F) The luminescent signals were detected in the abdomen of the mouse infected by Nipah pseudovirus.

showed that Doxycycline (Dox) treatment (1 μg/ml) induced expression of IFITM3 protein (Fig. 2A). The MDCK-Tet3G-IFITM3 cells were treated with DMSO or Dox and then infected with NiVpv and H5N9pv as a control. The luciferase expression was determined after 48 h of infection. The result showed that the fluorescence signal in the cells with Dox-induced IFITM3 expression was significantly enhanced compared with NiVpv-infected DMSO-treated cells (Fig. 2B), suggesting that IFITM3 had an enhancement effect on NiVpv-infected MDCK cells. On the contrary, Dox-induced IFITM3 inhibited the infection of H5N9pv to MDCK cells (Fig. 2C), which was consistent with the previous study (Majdoul and Compton, 2021). To confirm the effects of IFITM3 on the two pseudotypes above, targeted siRNA (5′ CCCACGUACUCCAACUUCC [dT][dT] 3′, BiboBio, China) was used to interfere with the Dox-induced IFITM3 expression, and a 38% decrease in the expression of IFITM3 was detected (Fig. 2D). Pseudotyped virus infection and reporter protein analysis showed that siRNA interference with IFITM3 expression resulted in a declined NiVpv infection, compared with Dox-induced cells treated with invalid siRNA (Fig. 2E), suggesting that IFITM3 enhanced NiVpv infection in MDCK cells. On the contrary, after siRNA interference with IFITM3 expression, the Luc signal in H5N9pv-infected cells was stronger than Dox-induced cells treated with invalid siRNA (Fig. 2F), indicating that reduced IFITM3 expression resulted in enhanced H5N9pv infection. Above all, IFITM3 can promote NiVpv infection to MDCK cells, which is significantly different from the inhibitory effect of IFITM3 on H5N9pv.

3.3. Direct interaction between IFITM3 and NiV F

Previous studies have proved that IFITM3 are mainly located in the late endosomes and lysosomes, but a small amount of IFITM3 is expressed on the plasma membrane (Compton et al., 2016, 2014). To investigate the mechanism by which IFITM3 promotes NiV G and F proteins-mediated virus entry, the subcellular distributions of the three proteins were first confirmed. The recombinant plasmid of NiV G or F fused with EGFP was constructed, and then co-transfected into BHK-21 cells with the plasmids carried organelle red fluorescent probe gene (Lck/ Rab5a/ Rab7/ LAMP1/ IFITM3/ HSPA5 and TGOLN2), respectively, and were observed by a confocal microscope after 48 h of transfection. The results showed that G protein was irregularly distributed in cells, without obvious co-localization with early endosomes (Rab5a), late endosomes (Rab7), lysosomes (LAMP1), IFITM3, endoplasmic reticulum (HSPA5), and Golgi (TGOLN2) (Fig. 3A). Although F protein had no obvious co-localization with early endosomes (Rab5a), it was completely co-localized with lysosomes (LAMP1) and IFITM3 and partial colocalization with late endosomes (Rab7) or Golgi (TGOLN2) (Fig. 3B). Thus, F protein was mainly located in late endosomes, lysosomes and Golgi, similar to IFITM3, suggesting a possible direct interaction between IFITM3 and F protein.

Next, the direct interaction between IFITM3 and NiV G and F protein was revealed by Co-IP. The results indicated that IFITM3 fusion protein captured NiV G, F0 protein, and F1 subunit, but GFP control protein was

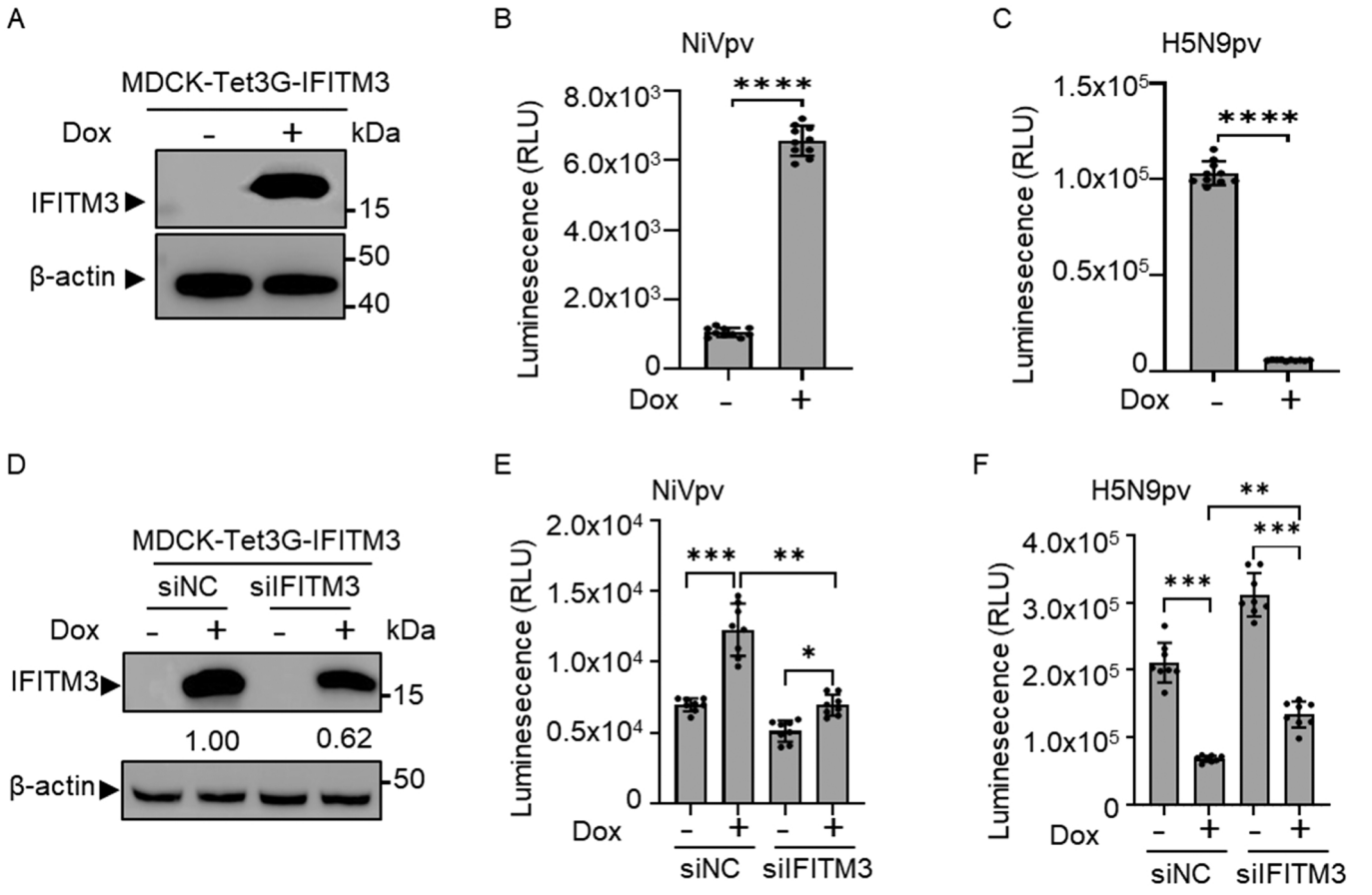

Fig. 2. Human IFITM3 promotes Nipah pseudovirus infections. (A)Treatment of MDCK-Tet3G-IFITM3 cells with Dox could express human IFITM3 protein compared with no-Dox, measured by Western blot with anti-IFITM3 antibody (Proteintech, China). Luminescence values of MDCK-Tet3G-IFITM3 treated with Dox or not and then infected by NiVpv (B) or H5N9 pv (C). The expression level of human IFITM3 decreased by about 38% when MDCK-Tet3G-IFITM3 cells were transfected with siIFITM3, compared to the treatment with siNC under Dox (D). The gray values of WB bands calculated by ImageJ software then normalized to siNC, set to 1.00. Cells as in (D) were infected with NiV pv (E) or H5N9 pv (F), then the luciferase activity was read at 48 h post-infection. Bars represent averages with individual data points from 8 to 10 independent experiments shown as dots. Error bars represent SD. *p*-values were determined by a two-tailed t-test. *** $p < 0.0001$; WB: Western blot.

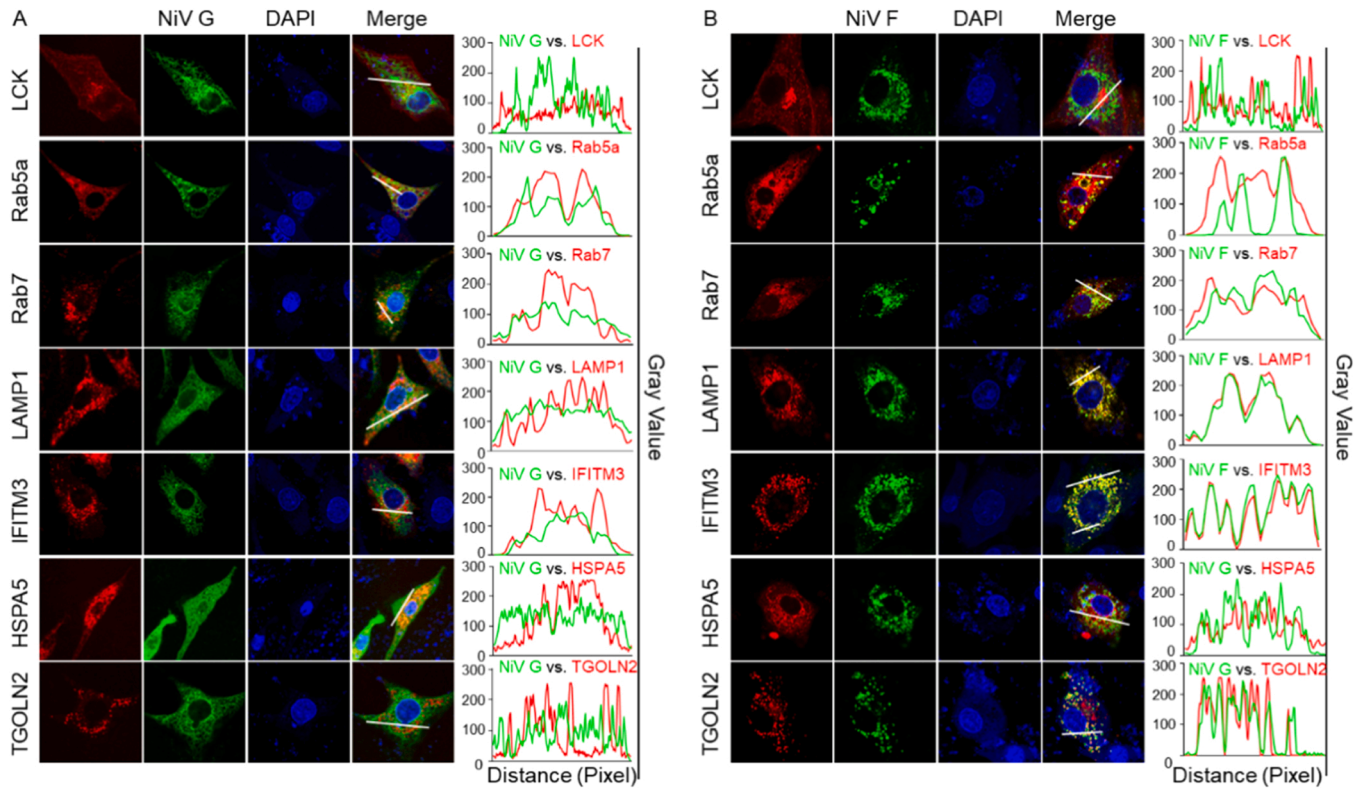

Fig. 3. Localization of NiV G and F protein. BHK cells were transfected with plasmid then observed by confocal laser scanning microscope (63 ×, oil). The NiV G (A) and F (B) genes were cloned into pEGFP-N3 (Green) , respectively. The organelle marker protein genes were inserted into pmCherry-N3 (Red). Co-localization of NiV G (A) or F (B) protein with the indicated cellular proteins was measured by the image processing program ImageJ. The fluorescence intensity value between 100 and 300 indicates no over-exposure when taking photos. The coincidence of the two lines is higher, the degree of co-location between them is greater. Lck: Cell membrane marker; Rab5a: Early endosome marker; Rab7: Late endosome marker; LAMP1: Lysosome marker; HSPA5: Endoplasmic reticulum marker; TGOLN2: Golgi marker.

not captured. IFITM3 fusion protein had a higher capability to capture F0 protein (Fig. 4), demonstrating that IFITM3 protein had a stronger affinity with F protein.

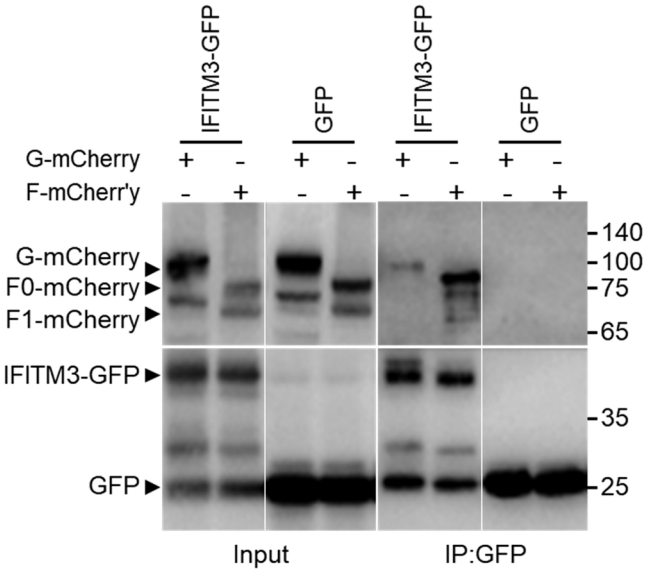

Fig. 4. Interaction of NiV G or F protein with IFITM3. The plasmid expressing the protein was transfected into 293 T cells. Co-immunoprecipitation experiments were performed with anti-GFP magnetic beads (Alpa-life, China). The anti-mCherry and anti-GFP antibodies (Abcam, USA) were used to Western blot.

3.4. Direct interaction between NiV F1 subunit and IFITM3

The synthesized NiV F0 glycoprotein has no activity, and is cleaved by cathepsin L into F1 and F2 subunits in the body, linked by disulfide bonds to form mature F glycoprotein (Weis and Maisner, 2015) (Fig. 5A). To study the interaction between IFITM3 and NiV F protein, truncated F1 and F2 were fused with GFP tag to construct recombinant plasmids. Then, BHK-21 cells were co-transfected with the IFITM3-mCherry plasmid and F1-GFP or F2-GFP plasmids, respectively, and observed by confocal microscope after 48 h of transfection. The results showed that the F1 subunit was completely co-localized with IFITM3, but the F2 subunit was not co-localized with it (Fig. 5B). The direct interaction between F1 or F2 and IFITM3 was further confirmed by Co-IP. The results indicated that F1 fusion protein captured IFITM3 fusion protein (Fig. 5C), but F2 protein could not capture it from cell lysates (Fig. 5D). In conclusion, IFITM3 directly interacts with the F1 subunit of F protein.

3.5. The important role of fusion peptide domain of F1 subunit in the interaction between IFITM3 and F1

The F1 subunit of F protein possesses multiple functional domains, such as fusion peptide region, a transmembrane region, two heptad repeat (HR) regions, intracellular region. (Fig. 6A). FP is a hydrophobic sequence rich in glycine on F protein, with membrane disturbance activity, and can be inserted into the lipid bilayer. The F1 subunit was truncated according to its functional domains (Fig. 6A) and cloned into pEGFP-N3 vector respectively to construct recombinants. Then, IFITM3-mCherry was co-transfected into 293 T cells together with these truncated plasmids, respectively. After 48 h of transfection, the cells were collected and lysed for Co-IP. The results showed that IFITM3 captured

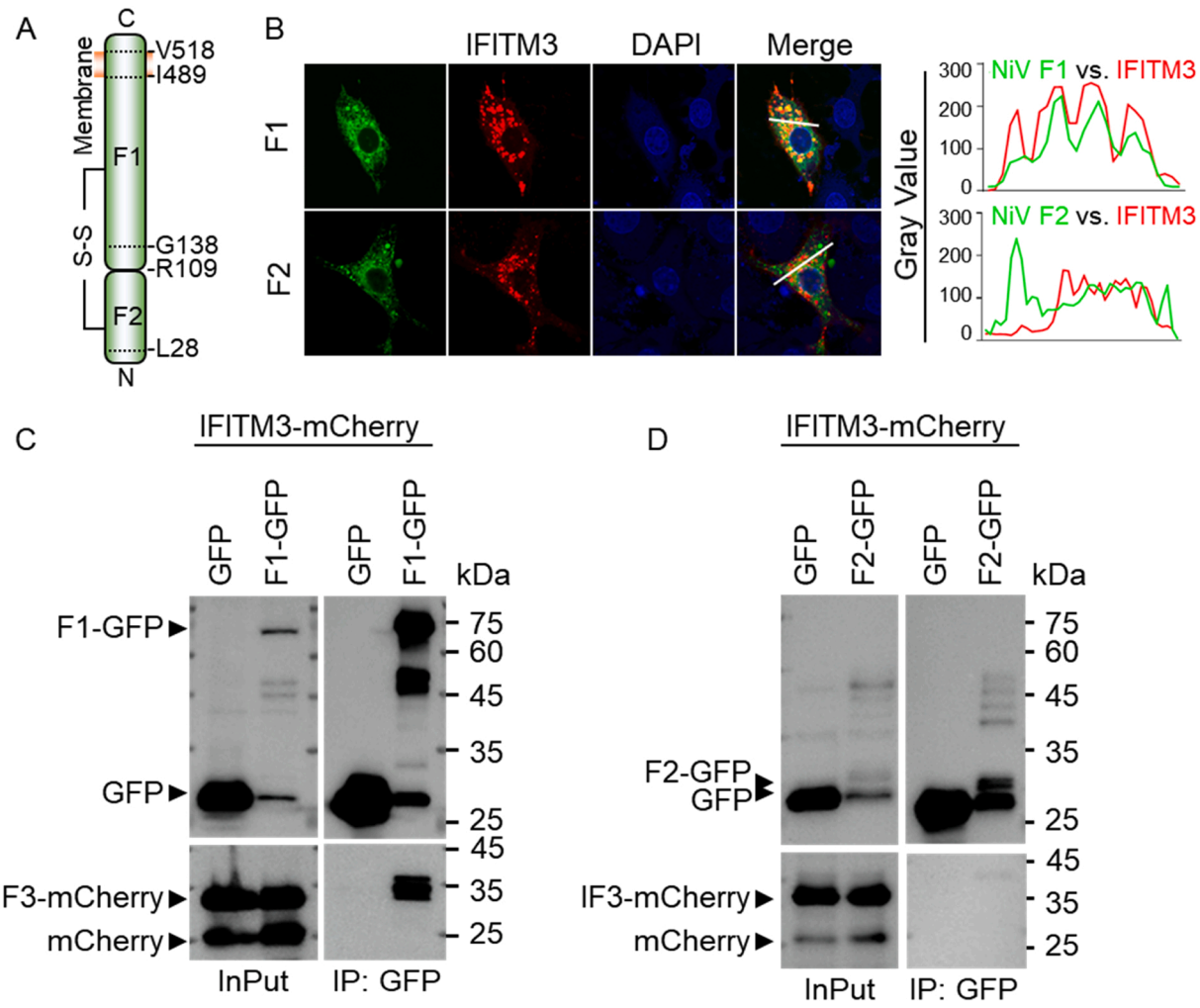

Fig. 5. Interaction of NiV F1 protein with IFITM3. (A) Schematic representation of the NiV F proteins. The orange part represents the virus envelopes. (B) Co-localization of NiV F1 (up, green) or F2 (down, green) proteins with IFITM3 (Red), respectively (63 ×, oil). The line graph on the right shows the fluorescence density values of pixels on the white line in the Merge. Co-immunoprecipitation (Co-IP) of NiV F1 (C) or NiV F2 (D) with IFITM3, respectively. Anti-GFP magnetic beads used for IP. Anti-GFP and anti-mCherry antibodies were used for Western blot.

F1 subunits and the truncated F1 fragment carried FP (aa110–448, aa110–489, and aa110–518), but not other truncated F1 (Fig. 6B). Thus, the fusion peptide domain of the F1 subunit plays a critical role for the interaction of IFITM3 with F1.

3.6. Intramembrane region of IFITM3 as a key domain for IFITM3-F1 interaction

IFITM3 is a single-pass transmembrane protein, including a free area in C-terminal and N-terminal, intracellular domain, intracellular ring, and transmembrane domain (Fig. 7A). To explore the key domain of IFITM3 interaction with F1, the previously constructed IFITM3 truncated fusion plasmids and F1-GFP fusion plasmids were used to co-transfect 293 T cells, respectively. After 48 h of transfection, the cells were collected and lysed for Co-IP. The results showed that the F1 fusion protein captured IFITM3-mCherry, IMD-mCherry, and TMD-mCherry fusion proteins in the precipitate, especially IMD fusion protein, IFITM3 NTD could not be captured (Fig. 7B), suggesting that IFITM3 IMD participated in the IFITM3-F1 interaction. Together, the IMD might be the critical domain of the interaction.

4. Discussion

Generally, although IFITM3 is considered with broad-spectrum antiviral activity, it also has no inhibitory effect on some viruses, such as human adenovirus type 5 (Ad5), human cytomegalovirus (hCMV), human tumor virus (HPV16), and other DNA viruses. It even has the function of promoting some infections. For example, Zhao et al. found that IFITM3 promoted HCoV OC43 to enter host cells via regulating the fusion of the HCoV OC43 envelope and cell membrane. Interestingly, IFITM3 has different effects on various paramyxoviruses. For example, IFITM3 can inhibit the early parainfluenza virus (PIV-3) infection to a certain extent, but does not effect the late infection. It can effectively inhibit the F protein-mediated human metapneumovirus (HMPV) type A1-cell membrane fusion, thus limiting the infection of hMPV to host cells, but has no significant effect on those infected by hMPV type A2 (McMichael et al., 2018). For Sendai virus (SeV), also belonging to paramyxoviridae, IFITM3 overexpression does not affect its infection to host cells (Jiang et al., 2018). Lv et al. found that IFITM3 inhibited the NDV infection in chicken embryos when treating the infection by Chinese herbal medicine formula. However, some studies also proved that the inhibitory effect of IFITM3 on the NDV infection to host cells was limited.

In this study, MDCK cell lines overexpressing IFITM3 were infected with NiVpv. It was found that the IFITM3 overexpression significantly promoted the NiVpv entry into host cells. Then, the expression level of IFITM3 was reduced by siRNA transfection, and the infection level of NiVpv was also significantly reduced, indicating that IFITM3 could

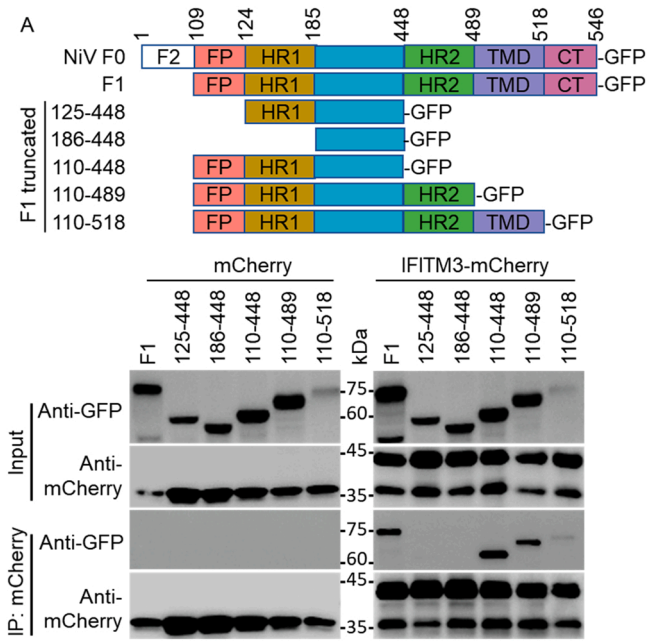

Fig. 6. IFITM3 interacts directly with NiV F1 subunit. (A) Schematic of NiV F. FP: fusion peptide; HR: heptad repeat region; TMD, transmembrane domain; CT, cytoplasmic tail; The different segments of the F protein were cloned into the pEGFP-N3 expression plasmid. (B) 293 T cells were transfected with the indicated plasmids, and then the cell lysates were used to Co-IP with anti-mCherry beads (Alpa-life, China) after 48 h. Anti-GFP and anti-mCherry antibodies were used to Western blot, respectively.

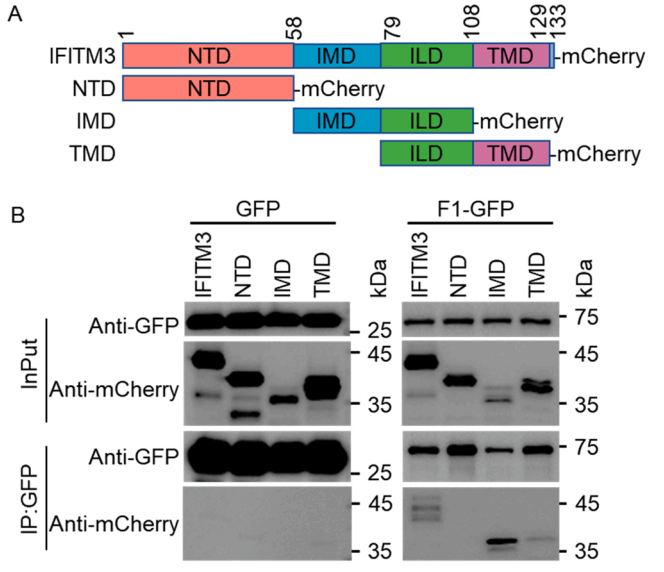

Fig. 7. NiV F1 subunit interacts with intramembrane region of IFITM3. (A) Schematic diagram of the IFITM3. NTD: N-terminal domain; IMD: intramembrane domain; ILD: intracellular loop domain; TMD: transmembrane domain. (B) Cell lysates of 293 T cells transfected with the indicated plasmids, were used for Co-IP. The anti-GFP and anti-mCherry antibody were used to Western blot.

promote NiVpv infection to host cells. This finding is different from the inhibitory effect of IFITM3 on RSV that also belongs to the *paramyxoviridae* (Zhang et al., 2015). IFITM3 blocks RSV from infecting host cells by inhibiting RSV and cell membrane fusion. However, unlike RSV, the co-regulation of G and F glycoproteins is necessary for NiV to infect host cells, but RSV does not necessarily need G protein during the entry to host cells (Techaarpornkul et al., 2002). NiV G protein is mainly responsible for the binding and recruitment of Ephrin-B2 or Ephrin-B3 receptors on the cell surface. The conformation change activates the F protein to start the membrane fusion. RSV G protein only plays an auxiliary role in viral infection to improve infection efficiency.

FP of NiV F protein is located on the F1 subunit, with a typical HR sequence and helical region (between HR1 and HR2) downstream (Fig. 6A). When the fusion peptide is inserted into the cell membrane, the fully unfolded HR1 region tilts toward the HR2 region to form fusion intermediates. After they are fully bound to form a stable fusion six-helix bundle (6HB), the viral envelope and cell membrane fuse to form fusion microporous release genomes (Wong et al., 2021). In this study, the NiV F protein and IFITM3 were truncated to express, respectively, and an obvious co-localization relationship between the whole F protein or F1 subunit and IFITM3 protein was shown in cells. And both of them were captured by IFITM3 via Co-IP, which indicates that IFITM3 interacted with F protein by binding the F1 subunit, similar to the influenza virus HA and HIV Env protein. However, IFITM3 inhibits the proliferation and transmission of HIV by preventing the maturation of HIV Env protein and reducing the number of HIV Env proteins in the viral envelope and MLV Env incorporation (Yu et al., 2015; Ahi et al., 2020).

Then, the F1 subunit and IFITM3 were truncated respectively in this study. The results of Co-IP indicated that IFITM3 interacted with a part of the fusion peptide of the NiV F1 subunit, and the NiV F1 subunit bound the intramembrane region (IMD) of IFITM3. Recent studies have shown that IFITM3 IMD (aa 59–68) is required for its inhibition of virus protein-mediated membrane fusion (Chesarino et al., 2017). Therefore, we speculated that IFITM3 took effects at the membrane fusion stage of NiV entry into MDCK cells. After the fusion peptide of F protein is inserted into the membrane, it stably binds to the intramembrane region of IFITM3 to make the fusion micropores easier to form and promote successful genome release of NiV. This finding has improved our understanding of the NiV pathogenesis and provided a new clue to the mechanism of NiV infection.

5. Conclusions

In conclusion, we found that overexpression of IFITM3 can promote NiV G and F proteins-mediated virus entry into MDCK cells, and IFITM3 directly interacts with the F1 subunit of NiV F protein, which is caused by the interaction between the IMD of IFITM3 and the FP of F1, which may occur after incorporation of fusion peptides into the cell membrane following virus fusion activation. This study will provide a new idea and direction for investigating the mechanisms or drugs against NiV infection.

CRediT authorship contribution statement

Wang Xu: Investigation, Methodology, Writing – original draft. **Shou-Wen Du:** Formal analysis, Investigation, Data curation, Validation. **Le-Tian Li:** Validation, Data curation. **Xiao-Shuang Shi:** Investigation. **Jia-Min Wang**: Investigation. **Ti-Yuan Li**: Data curation. **Ning-Yi Jin:** Supervision, Visualization, Funding acquisition. **Chang Li:** Conceptualization, Formal analysis, Data curation, Validation, Writing – original draft, Supervision, Project administration, Funding acquisition. All authors checked the final version of the manuscript.

Data Availability

No data was used for the research described in the article.

Acknowledgements

This work was supported by the National Key Research and Development Program of China (2021YFD1801103), the National Natural Science Foundation of China (31972719), and the CAMS Innovation

Fund for Medical Sciences (2020–12M-5–001).

Appendix A. Supporting information

Supplementary data associated with this article can be found in the online version at doi:10.1016/j.biocel.2022.106325.

References

Ahi, Y.S., Yimer, D., Shi, G., Majdoul, S., Rahman, K., Rein, A., Compton, A.A., 2020. IFITM3 reduces retroviral envelope abundance and function and is counteracted by glycoGag. mBio 11 (1) e03088-19.

Cao, T.T., Du, S.W., Xu, W., Xing, B., Zhao, F., Wang, M.P., et al., 2017. Establishment and functional analysis of MDCK Cell Line Induced IFITM3 Expression Based on Tet-On 3G System. Chem. J. Chin. Univ. 38, 770–777.

Chesarino, N.M., Compton, A.A., McMichael, T.M., Kenney, A.D., Zhang, L., Soewarna, V., et al., 2017. IFITM3 requires an amphipathic helix for antiviral activity. EMBO Rep. 18 (10), 1740–1751.

Chua, K.B., Wong, E.M., Cropp, B.C., Hyatt, A.D., 2007. Role of electron microscopy in Nipah virus outbreak investigation and control. Med. J. Malays. 62, 139–142.

Compton, A.A., Bruel, T., Porrot, F., Mallet, A., Sachse, M., Euvrard, M., et al., 2014. IFITM proteins incorporated into HIV-1 virions impair viral fusion and spread. Cell Host Microbe 16 (6), 736–747.

Compton, A.A., Roy, N., Porrot, F., Billet, A., Casartelli, N., Yount, J.S., et al., 2016. Natural mutations in IFITM3 modulate post-translational regulation and toggle antiviral specificity. EMBO Rep. 17 (11), 1657–1671.

Guo, X., Steinkühler, J., Marin, M., Li, X., Lu, W., Dimova, R., et al., 2020. Interferon-induced transmembrane protein 3 blocks fusion of diverse enveloped viruses by locally altering mechanical properties of cell membranes. Biophys. J. 120, 320a.

Hauser, N., Gushiken, A.C., Narayanan, S., Kottilil, S., Chua, J.V., 2021. Evolution of nipah virus infection: past, present, and future considerations. Trop. Med. Infect. Dis. 6, 24.

Isaacs, A., Cheung, S.T.M., Thakur, N., Jaberolansar, N., Young, A., Modhiran, N., et al., 2021. Combinatorial F-G immunogens as nipah and respiratory syncytial virus vaccine candidates. Viruses 13, 13.

Jiang, L.Q., Xia, T., Hu, Y.H., Sun, M.S., Yan, S., Lei, C.Q., et al., 2018. IFITM3 inhibits virus-triggered induction of type I interferon by mediating autophagosome-dependent degradation of IRF3. Cell Mol. Immunol. 15, 858–867.

Li, C., Du, S., Tian, M., Wang, Y., Bai, J., Tan, P., et al., 2018. The host restriction factor interferon-inducible transmembrane protein 3 inhibits vaccinia virus infection. Front Immunol. 9, 228.

Liu, Q., Stone, J.A., Bradel-Tretheway, B., Dabundo, J., Benavides Montano, J.A., Santos-Montanez, J., et al., 2013. Unraveling a three-step spatiotemporal mechanism of triggering of receptor-induced Nipah virus fusion and cell entry. PLoS Pathog. 9, e1003770.

Lv, W., Liu, C., Zeng, Y., Li, Y., Chen, W., Shi, D., et al., 2019. Explore the potential effect of natural herbals to resist newcastle disease virus. Poult. Sci. 98, 1993–1999.

Majdoul, S., Compton, A.A., 2021. Lessons in self-defence: inhibition of virus entry by intrinsic immunity. Nat. Rev. Immunol. 1–14.

McMichael, T.M., Zhang, Y., Kenney, A.D., Zhang, L., Zani, A., Lu, M., et al., 2018. IFITM3 restricts human metapneumovirus infection. J. Infect. Dis. 218, 1582–1591.

Meischel, T., Fritzlar, S., Villalon-Letelier, F., Tessema, M.B., Londrigan, S.L., 2021. IFITM proteins that restrict the early stages of respiratory virus infection do not influence late-stage replication. J. Virol.

Nie, J., Liu, L., Wang, Q., Chen, R., Ning, T., Liu, Q., et al., 2019. Nipah pseudovirus system enables evaluation of vaccines in vitro and in vivo using non-BSL-4 facilities. Emerg. Microbes Infect. 8, 272–281.

Pernet, O., Pohl, C., Ainouze, M., Kweder, H., Buckland, R., 2009. Nipah virus entry can occur by macropinocytosis. Virology 395, 298–311.

Prelli Bozzo, C., Nchioua, R., Volcic, M., Koepke, L., Kruger, J., Schutz, D., et al., 2021. IFITM proteins promote SARS-CoV-2 infection and are targets for virus inhibition in vitro. Nat. Commun. 12, 4584.

Ren, L., Du, S., Xu, W., Li, T., Wu, S., Jin, N., et al., 2020. Current progress on host antiviral factor IFITMs. Front Immunol. 11, 543444.

Smith, S.E., Busse, D.C., Binter, S., Weston, S., Diaz Soria, C., Laksono, B.M., et al., 2019. Interferon-induced transmembrane protein 1 restricts replication of viruses that enter cells via the plasma membrane. J. Virol. 93.

Techaarpornkul, S., Collins, P.L., Peeples, M.E., 2002. Respiratory syncytial virus with the fusion protein as its only viral glycoprotein is less dependent on cellular glycosaminoglycans for attachment than complete virus. Virology 294, 296–304.

The L. Nipah virus control needs more than R&D. The Lancet. 2018; 391: 2295.

Weis, M., Maisner, A., 2015. Nipah virus fusion protein: Importance of the cytoplasmic tail for endosomal trafficking and bioactivity. Eur. J. Cell Biol. 94, 316–322.

Welch, S.R., Chakrabarti, A.K., Wiggleton Guerrero, L., Jenks, H.M., Lo, M.K., Nichol, S. T., et al., 2018. Development of a reverse genetics system for Sosuga virus allows rapid screening of antiviral compounds. PLoS Negl. Trop. Dis. 12, e0006326.

Wong, J.J., Chen, Z., Chung, J.K., Groves, J.T., Jardetzky, T.S., 2021. EphrinB2 clustering by Nipah virus G is required to activate and trap F intermediates at supported lipid bilayer-cell interfaces. Sci. Adv. 7 eabe1235.

Yanez, D.C., Ross, S., Crompton, T., 2020. The IFITM protein family in adaptive immunity. Immunology 159, 365–372.

Yeo, Y.Y., Buchholz, D.W., Gamble, A., Jager, M., Aguilar, H.C., 2021. Headless henipaviral receptor binding glycoproteins reveal fusion modulation by the head/stalk interface and post-receptor binding contributions of the head domain. J. Virol. 95, e0066621.

Yu, J., Li, M., Wilkins, J., Ding, S., Swartz, T.H., Esposito, A.M., et al., 2015. IFITM proteins restrict HIV-1 infection by antagonizing the envelope glycoprotein. Cell Rep. 13, 145–156.

Zamora, J.L.R., Ortega, V., Johnston, G.P., Li, J., Aguilar, H.C., 2021. Novel roles of the N1 Loop and N4 alpha-helical region of the nipah virus fusion glycoprotein in modulating early and late steps of the membrane fusion cascade. J. Virol. 95 e01707-20.

Zhang, W., Zhang, L., Zan, Y., Du, N., Yang, Y., Tien, P., 2015. Human respiratory syncytial virus infection is inhibited by IFN-induced transmembrane proteins. J. Gen. Virol. 96, 170–182.